



A novel online two-dimensional supercritical fluid chromatography/reversed phase liquid chromatography–mass spectrometry method for lipid profiling

Li Yang^{1,2} · Honggang Nie³ · Fan Zhao¹ · Shiyao Song¹ · Ying Meng⁴ · Yu Bai¹ · Huwei Liu¹

Received: 21 July 2019 / Revised: 22 October 2019 / Accepted: 28 October 2019 / Published online: 4 January 2020
© Springer-Verlag GmbH Germany, part of Springer Nature 2020

Abstract

A novel online two-dimensional supercritical fluid chromatography/reversed-phase liquid chromatography–triple-quadrupole mass spectrometry (2D SFC/RPLC–QQQ MS) method based on a vacuum solvent evaporation interface was developed for lipid profiling in human plasma, in which lipid classes were separated by the first-dimension SFC and different lipid molecular species were further separated by the second-dimension RPLC. All separation condition parameters were carefully optimized, and their influence on the chromatographic behavior of lipids is discussed. Finally, the recoveries of 11 lipid standards were all more than 88% for the interface. Besides, the limit of detection for these lipid standards was on the order of nanograms per milliliter, and the relative standard deviations of the peak area and retention time ranged from 1.54% to 19.85% and from 0.00% to 0.10%, respectively. The final 2D SFC/RPLC–QQQ MS method allowed the identification of 370 endogenous lipid species from ten lipid classes, including diacylglycerol, triacylglycerol, ceramide, glucosylceramide, galactosylceramide, lactosylceramide, sphingomyelin, acylcarnitine, phosphatidylcholine, and lysophosphatidylethanolamine, in human plasma within 38 min, which was used for screening potential lipid biomarkers in breast cancer. The 2D SFC/RPLC–QQQ MS method is a potentially useful tool for in-depth studies focused on complex lipid metabolism and biomarker discovery.

Keywords Lipidomics · Two-dimensional · Supercritical fluid chromatography · Mass spectrometry

Published in the topical collection *Current Progress in Lipidomics* with guest editors Michal Holčápek, Gerhard Liebisch, and Kim Ekroos.

Electronic supplementary material The online version of this article (<https://doi.org/10.1007/s00216-019-02242-x>) contains supplementary material, which is available to authorized users.

✉ Huwei Liu
hwliu@pku.edu.cn

¹ Beijing National Laboratory for Molecular Sciences, Key Laboratory of Bioorganic Chemistry and Molecular Engineering of Ministry of Education, Institute of Analytical Chemistry, College of Chemistry and Molecular Engineering, Peking University, Zhongguancun Street, Beijing 100871, China

² College of Pharmacy, Shanxi Medical University, Taiyuan 030001, Shanxi, China

³ Analytical Instrumentation Center, Peking University, Beijing 100871, China

⁴ Agilent Technologies, 3 Wangjing North Road, Beijing 100102, China

Introduction

Lipids are hydrophobic or amphiphilic small molecules that play crucial roles in cellular energy storage, structure, and signaling [1]. According to their structures, they can be divided into eight categories, and then into different classes and molecular species [2]. As changes in lipid metabolism and function have important effects on cellular physiological functions and pathological disorders of living organisms, lipidomics has attracted more and more attention in recent years [3]. However, there are still challenges associated with the analytical techniques used in lipidomics because of the extreme structural and content diversity of lipids in real biological samples.

Currently, two main analytical strategies are used in lipidomics; namely, shotgun lipidomics and high-performance liquid chromatography (HPLC)–mass spectrometry (MS) [4]. In general, shotgun lipidomics is considered to be of high throughput, accurate, and

highly sensitive. However, discrimination of some lipid isomers is a challenge for this method. Besides, identification of low-abundance or less-ionizable lipids is also difficult because of possible ion suppression [5]. Compared with shotgun lipidomics, HPLC–MS usually provides more comprehensive information about the lipid composition. Because of the chromatographic separation before MS, HPLC–MS can avoid ion suppression to some extent, and it is possible to separate lipid isomers. At present, two main modes of HPLC are used to separate lipids: normal phase liquid chromatography (NPLC) and reversed-phase liquid chromatography (RPLC). NPLC allows the separation of lipids into lipid classes according to their polarity, whereas RPLC is widely used for the separation of individual lipid species according to the carbon number and the double-bond number [6, 7]. Therefore, NP/RP two-dimensional (2D) liquid chromatography (LC)–MS has significant advantages in lipid analysis, as the orthogonal system can enhance the resolving power and provide a higher peak capacity. In our previous work, an online NP/RP 2D LC–MS method was developed on the basis of a solvent evaporation interface for comprehensive lipid profiling, and this could realize the analysis of more than 500 lipid species from 17 lipid classes [8–10]. However, the analysis time was rather long (nearly 3 h).

In recent years, supercritical fluid chromatography (SFC) has shown great potential as a comprehensive and high-throughput screening method in different omic fields, including lipidomics. Compared with traditional LC, SFC has met with great favor in lipid profiling because of its high efficiency, low organic solvent consumption, and its unambiguous identification of some isomeric lipids [11]. SFC–MS has been used for targeted lipid profiling, including profiling of phospholipids [12], sphingolipids [13], fatty acids [14], triacylglycerols (TGs) [15], and prenol lipids [16]. As the separation mechanism of SFC using polar stationary phases is similar to that of NPLC [17], the combination of SFC and RPLC could also achieve a high degree of orthogonality and maximize the effective 2D peak capacity. Besides, the analysis time could be significantly reduced compared with that of NP/RP 2D LC–MS method. The potential of RPLC \times SFC has been highlighted by Stevenson et al. [18] in off-line mode. Online comprehensive RPLC \times SFC was first investigated by Sarrut et al. [19] for bio-oil analysis using traditional sample loops as the interface. More recently, Sun et al. [20] introduced a trapping column interface for the analysis of depolymerized lignin samples. Besides, selective comprehensive 2D RPLC \times SFC was also investigated for the analysis of chiral pharmaceutical compounds [21]. According to the

classification and structure of lipids, SFC \times RPLC is more suitable for the analysis of lipids. The potential of SFC as the first dimension in an online RPLC \times SFC system with a trapping column interface was demonstrated by François and Sandra [22]. However, only fatty acids were analyzed.

In the present study, we aimed to develop a novel 2D SFC/RPLC—triple-quadrupole (QQQ) MS method for analysis of lipids, including monoacylglycerol (MG), diacylglycerol (DG), TG, ceramide (Cer), glucosylceramide (GluCer), galactosylceramide (GalCer), lactosylceramide (LacCer), sphingomyelin (SM), lysophosphatidylethanolamine (LPE), phosphatidylcholine (PC), and acylcarnitine (AC), in complex biological samples based on a ten-port, two-position vacuum evaporation interface. The potential of this lipidomic method is demonstrated by the analysis of lipid extract from human plasma.

Materials and methods

Reagents and materials

Chloroform (HPLC grade) was purchased from Mallinckrodt Baker (Phillipsburg, NJ, USA). HPLC grade *n*-hexane, 2-propanol, and methanol as well as ammonium formate (purity 99.995% or greater), were obtained from Sigma-Aldrich (St Louis, MO, USA). Purified water was acquired from Hangzhou Wahaha Group Co. (Zhejiang, China). All lipid standards, including 1-(10Z-heptadecenoyl)-*sn*-glycero-3-phosphoethanolamine [LPE (17:1)], 1,2-dimyristelaidoyl-*sn*-glycero-3-phosphocholine [PC (14:1/14:1)], *N*-lauroyl-D-*erythro*-sphingosine [Cer (d18:1/12:0)], D-galactosyl- β -1,1'-*N*-octanoyl-D-*erythro*-sphingosine [GalCer (d18:1/8:0)], D-glucosyl- β -1,1'-*N*-lauroyl-D-*erythro*-sphingosine [GluCer (d18:1/12:0)], D-lactosyl- β -1,1'-*N*-octanoyl-D-*erythro*-sphingosine [LacCer (d18:1/8:0)], *N*-(heptadecanoyl)-sphing-4-enine-1-phosphocholine [SM (d18:1/17:0)], 1-heptadecanoyl-*rac*-glycerol [MG (17:0)], 1,2-dilauroyl-*sn*-glycerol [DG (12:0/12:0)], 1-(9Z-octadecenoyl)-2-tetradecanoyl-3-(10Z-heptadecenoyl)-*sn*-glycerol [TG (18:1/14:0/17:1)], and palmitoyl D-carnitine [AC (16:0)] were purchased from Avanti Polar Lipids (Alabaster, AL, USA). Stock solutions of individual lipid standard at a concentration of 1 mg/mL were prepared in Folch solution (chloroform–methanol, 2:1 v/v). Lipid standard mixture contained all lipid standards with a concentration of 1 μ g/mL. Calibration solutions were prepared by the dilution of lipid standard mixture in a hexane–2-propanol mixture (1:1 v/v). Human plasma samples from ten patients with breast cancer and ten healthy controls were included in this study. For breast tumor, it could be easily recognized by

touch. However, we can't distinguish between benign breast tumor and breast cancer. Thus, the tumor should be confirmed by visual inspection of stained tissue by an experienced pathologist. This study was approved by the Ethics Committee of the Fifth Medical Center of the People's Liberation Army General Hospital (previously the Affiliated Hospital of the Academy of Military Medical Sciences). Lipids were extracted from human plasma by a modified Folch extraction method [23]. Before analysis, the dried lipid extracts were redissolved in 500 μL of Folch solution.

Two-dimensional SFC/RPLC–QQQ MS conditions

Two-dimensional SFC/RPLC system

The 2D SFC/RPLC system was based on a ten-port, two-position valve (Agilent Technologies, Santa Clara, CA, USA) vacuum evaporation interface reported previously [24] with some modification (Fig. 1). The mobile phase from the SFC column in the first dimension was evaporated by a vacuum pump when it flowed through the loops. By automatic switching of the valve, the two loops were used to trap analytes and transfer them to the second dimension alternately, and thus a nonstop-flow 2D SFC/RPLC system was realized. These two loops (0.12-mm inner diameter \times 50 mm and 0.02 in. \times 100 mm stainless steel pipeline for each loop) were maintained at 50 $^{\circ}\text{C}$ by a homemade

electrically heated thermostatic oil bath. An RV3 pump (Edwards, Crawley, UK) was used to evaporate the first-dimension solvent and trap analytes in loops.

The first-dimension SFC was performed with a 1260 series SFC system (Agilent Technologies, Santa Clara CA, USA). The final SFC method used the following conditions: two Zorbax RX-SIL columns (2.1 mm \times 150 mm, 5 μm ; Agilent Technologies, Santa Clara, CA, USA); column temperature, 40 $^{\circ}\text{C}$; flow rate, 0.4 mL/min; mobile phase A1, supercritical CO_2 ; mobile phase B1, methanol–water mixture (500:10 v/v) containing 20 mM ammonium formate; injection volume, 5 μL ; backpressure regulator (BPR) pressure, 160 bar; BPR temperature, 60 $^{\circ}\text{C}$. The first-dimension SFC instrument was connected with a valve via a commercial kit (Agilent) composed of T-pieces allowing backpressure control and mixing of column effluent with makeup liquid. Methanol containing 5 mM ammonium formate delivered by a quaternary pump (Agilent) was used as the makeup liquid. In the second dimension, a 1290 II series RPLC system consisting of a binary pump and a thermostated column compartment (Agilent Technologies, Santa Clara, CA, USA) was utilized. The second-dimension separation was performed on a Poroshell 120 EC C_8 column (2.1 mm \times 50 mm, 2.7 μm ; Agilent Technologies, Santa Clara, CA, USA). The

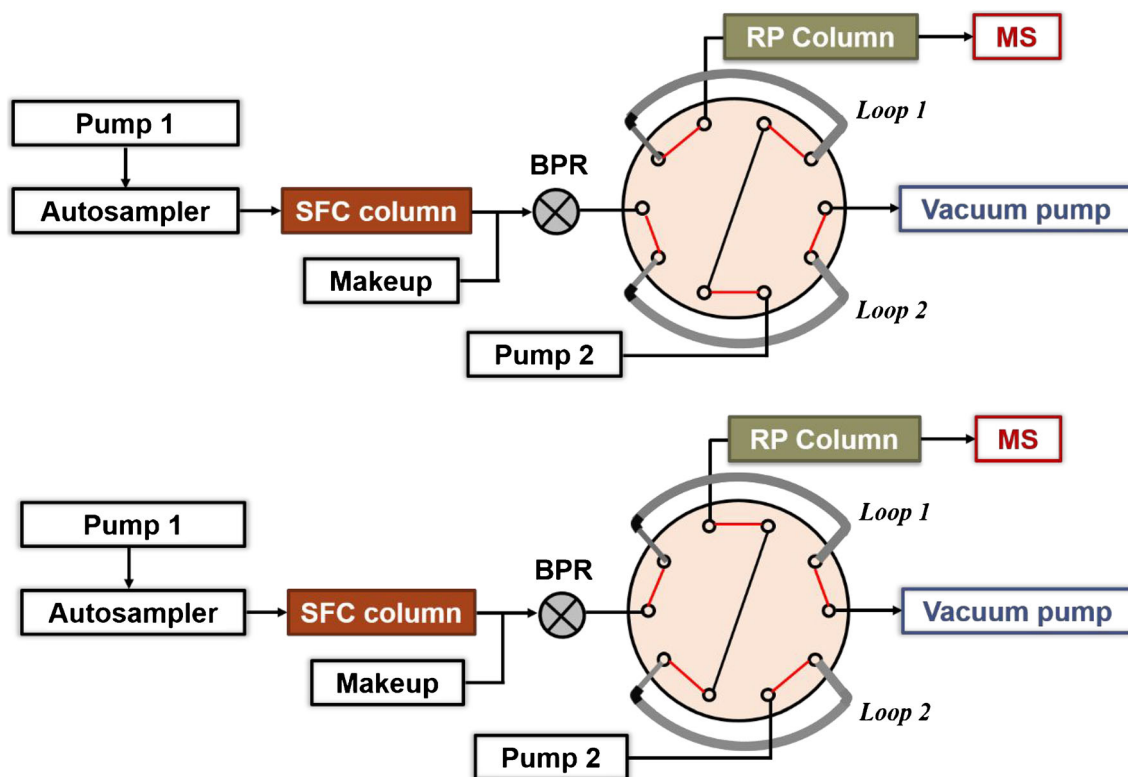


Fig. 1 The two-dimensional supercritical fluid chromatography (SFC)/reversed-phase (RP) liquid chromatography–mass spectrometry system based on a ten-port, two-position valve. BPR backpressure regulator, MS mass spectrometer

column temperature was 40 °C and the flow rate was 0.6 mL/min. Mobile phases A2 and B2 were water and methanol, both containing 10 mM ammonium formate.

The gradient programs for both dimensions and the valve switching program at the final condition are described in Table 1.

Table 1 Configuration of the online two dimensional supercritical fluid chromatography (SFC)/reversed-phase liquid chromatography (RPLC)–mass spectrometry system

First-dimension SFC			Makeup liquid		Interface	Second-dimension RPLC		
<i>t</i> (min)	A1 (%)	B1 (%)	<i>t</i> (min)	Flow rate (mL/min)	Loop/position	<i>t</i> (min)	A2 (%)	B2 (%)
0.00	90.00	10.00	0.00	0.25	1	0.00	30.00	70.00
			3.80	0.25	2	3.80	30.00	70.00
			3.81	0.20				
						4.10	0.00	100.00
						5.90	0.00	100.00
						5.91	30.00	70.00
			6.60	0.20	1	6.60	30.00	70.00
			6.61	0.15				
						6.90	0.00	100.00
						8.65	0.00	100.00
						8.66	30.00	70.00
			9.30	0.15				
			9.31	0.00				
					2	9.35	30.00	70.00
						9.85	0.00	100.00
						11.20	0.00	100.00
						11.21	30.00	70.00
					1	11.90	30.00	70.00
						12.40	0.00	100.00
						13.70	0.00	100.00
						13.71	30.00	70.00
					2	14.40	30.00	70.00
						14.90	30.00	70.00
						16.40	0.00	100.00
17.00	40.00	60.00						
17.01	0.00	100.00						
						19.20	0.00	100.00
						19.21	30.00	70.00
					1	19.90	30.00	70.00
						20.40	30.00	70.00
						21.90	0.00	100.00
						24.40	0.00	100.00
						24.41	30.00	70.00
					2	25.40	30.00	70.00
						25.90	30.00	70.00
						27.90	0.00	100.00
30.00	0.00	100.00	30.00	0.00				
30.01	90.00	10.00	30.01	0.25				
						36.50	0.00	100.00
						36.51	30.00	70.00
38.00	90.00	10.00	38.00	0.25		38.00	30.00	70.00

A1 supercritical CO₂, A2 water containing 10 mM ammonium formate, B1 methanol–water mixture (500:10 v/v) containing 20 mM ammonium formate, B2 methanol containing 10 mM ammonium formate

Mass spectrometry

In this 2D SFC/RPLC–MS system, the second-dimension RPLC system was coupled online to an Agilent 6470 QQQ mass spectrometer, with the eluate from the second-dimension column flowing directly into the electrospray ionization source. QQQ MS was performed in positive ion mode, and the instrument parameters were set as follows: sheath gas temperature, 325 °C; sheath gas flow rate, 11 L/min; nebulizer pressure, 45 psi; gas temperature, 325 °C; gas flow rate, 6 L/min; capillary entrance voltage, 3500 V; electron multiplier voltage, 300 V; nozzle voltage, 1500 V. Mass spectrometry data were acquired by multiple reaction monitoring (MRM) scan.

Recovery at the interface

To study the recovery rate of lipids at the interface, we used a six-port, two-position valve on the thermostated column compartment before the interface. During the analysis, one injection was directly analyzed by one-dimensional (1D) SFC without trapping by the loops, and another injection was trapped by the loops and then transferred to the SFC column for analysis (see Fig. S1). Finally, the recovery of each lipid standard was calculated by the ratio of the two peak areas.

Method validation

The linearity, limit of detection (LOD), and repeatability of the 2D SFC/RPLC–QQQ MS method were determined. The calibration curves for this method were constructed for 11 lipid standards, including LPE (17:1), PC (14:1/14:1), Cer (d18:1/12:0), GalCer (d18:1/8:0), GluCer (d18:1/12:0), LacCer (d18:1/8:0), SM (d18:1/17:0), MG (17:0), DG (12:0/12:0), TG (18:1/14:0/17:1), and AC (16:0), with concentrations of 0.0001, 0.0002, 0.0005, 0.001, 0.002, 0.005, 0.01, 0.02, 0.05, 0.1, 0.2, 0.5, and 1 µg/mL. The linearity was determined from calibration curves plotted as peak area versus concentration of lipid standard solutions and calculated by linear regression. Each calibration point was measured in quadruplicate. The LOD was determined from a signal-to-noise ratio of 3. For repeatability, the relative standard deviations (RSDs) of the peak area and retention time of each lipid standard were calculated on the basis of six consecutive injections of the same concentration (1 µg/mL) of 11 lipid standards.

Data processing

MS data were processed by the MassHunter Qualitative Analysis B.07.00 (Agilent Technologies, Santa Clara, CA, USA). All MRM chromatograms were obtained with ± 0.5 *m/z* expansion. Peak areas of each individual lipid species were corrected by the peak area of an internal standard

corresponding to the same lipid class or in the same fraction for each sample. Then the corrected peak areas were used for statistical analysis by the Mann–Whitney *U* test by IBM SPSS Statistics, version 20 (IBM, Armonk, NY, USA). Differences were considered to be significant if *p* was less than 0.05. Besides, the fold change was calculated from the arithmetic means of the healthy control and patient groups. Origin 2016 (OriginLab, Northampton, MA, USA) was used for visualization of lipid recovery under different interface conditions.

Results and discussion

Optimization of MRM transition settings for lipid standards

Identification of the precursor ions and elucidation of the fragmentation patterns of each lipid standard were performed by direct infusion analysis. Precursor ions of each lipid were clearly observed in the positive ion mode by $[M + H]^+$ or $[M + NH_4]^+$. Tandem MS (MS/MS) spectra of the individual lipid precursor ions, which could produce signature product ions specific for each molecular substructure, were acquired by collision-induced dissociation with nitrogen. On the basis of the most abundant adduct precursor ion and the selected product ion for each lipid, we optimized the MS fragmentor voltage and collision energy. The optimized acquisition settings, including precursor–product ion pairs, fragmentor voltage, and collision energy, are presented in Table S1.

Optimization of the 2D SFC/RPLC system interface

As mentioned before, a ten-port, two-position valve with two loops was used as the interface of the 2D SFC/RPLC system. Compared with the NP/RP 2D LC system, the combination of SFC and RPLC using a vacuum solvent evaporation interface should be better. As the mobile phase from the first-dimension SFC contains a large amount of supercritical CO₂, which will change to CO₂ gas after backpressure regulation, the viscosity of the solvent vapor is lower and the pressure at the solution front is higher, leading to a faster evaporation rate. Before the interface was used to trap the first-dimension eluate and transfer it to the second dimension, the conditions for the interface were optimized. The temperature of oil bath, in which the loops were maintained at constant temperature, was studied under three conditions (30, 50, and 70 °C). Besides, different flow rates of the mobile phase (0.2, 0.3, 0.4, 0.5, and 0.6 mL/min) were also investigated to achieve the greatest recovery of lipids.

According to a previous report [25], raising the temperature and increasing the flow rate of the mobile phase can increase the evaporation rate. A higher evaporation rate is good for the evaporation of the mobile phase, which can increase the recovery at the interface. However, when the evaporation rate is

too high, it will cause loss of samples, resulting in a decrease of recovery at the interface. Therefore, the interface recovery initially increases with increase of temperature and flow rate of the mobile phase, but decreases with further increase of them. As shown in Fig. 2, the results of the optimization experiment were consistent with our expectation.

After optimization, 50 °C and 0.4 mL/min were chosen as the temperature of the oil bath and the flow rate of first-dimension mobile phase, respectively. Under these conditions, the recoveries of 11 lipid standards were all more than 88%, as shown in Table 2.

Two-dimensional SFC/RPLC–MS method development

We aimed to develop a nonstop-flow 2D SFC/RPLC–MS method, in which the first-dimension SFC is used to separate lipid classes by the difference in their polarity, and the second-dimension RPLC is used to separate the lipid molecular species according to their different acyl chains, for the analysis of lipids, including MG, DG, TG, Cer, GluCer, GalCer, LacCer, SM, LPE, PC, and AC, in human plasma. For this purpose, a column with silica stationary phase was selected for lipid class separation in the first-dimension SFC and a short Poroshell 120 EC C₈ column was selected for fast separation of lipid molecular species in the second-dimension RPLC. As lipid class separation in the first dimension is particularly important for the 2D method, individual parameters of the SFC separation were carefully optimized, including BPR pressure, column temperature, and flow rates of the mobile phase and the makeup liquid, with a lipid standard mixture.

We found that the retention times of the lipids increased with increase of BPR pressure (Fig. S2). Besides, the influence of column temperature was not consistent for different lipids. As shown in Fig. S3,

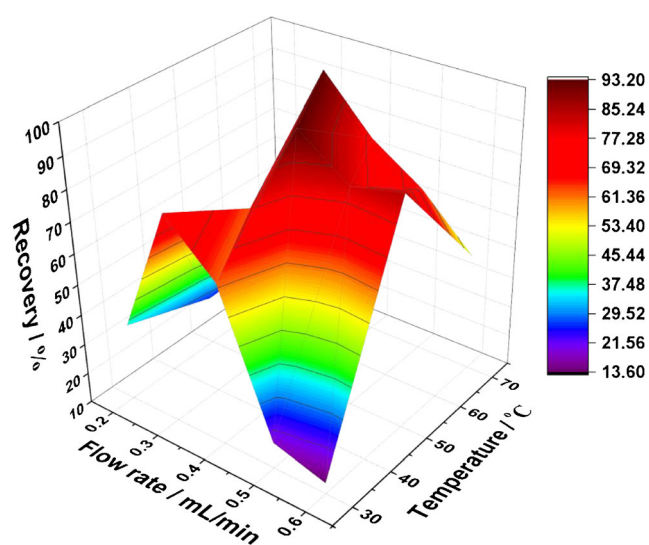


Fig. 2 Recovery of diacylglycerol (12:0/12:0) under different interface conditions

Table 2 Recovery of 11 lipid standards when the oil bath temperature was 50 °C and the flow rate of first-dimension mobile phase was 0.4 mL/min

Lipid standard	Recovery (%)
MG (17:0)	107
DG (12:0/12:0)	93.2
TG (18:1/14:0/17:1)	110
Cer (d18:1/12:0)	110
GalCer (d18:1/8:0)	116
GluCer (d18:1/12:0)	108
LacCer (d18:1/8:0)	111
SM (d18:1/17:0)	89.4
LPE (17:1)	119
PC (14:1/14:1)	88.3
AC (16:0)	91.3

AC acylcarnitine, *Cer* ceramide, *DG* diacylglycerol, *GalCer* galactosylceramide, *GluCer* glucosylceramide, *LacCer* lactosylceramide, *LPE* lysophosphatidylethanolamine, *MG* monoacylglycerol, *PC* phosphatidylcholine, *SM* sphingomyelin, *TG* triacylglycerol

for lipids with a retention time of less than 12 min, the retention time increased with increase of the column temperature. But for lipids with a retention time of more than 22 min, the retention time decreased with increase of the column temperature. Because of the large increase of the organic phase concentration during analysis, the mobile phase changed from the supercritical fluid to subcritical fluid and then to organic fluid. For conventional LC with an organic liquid as the mobile phase, the retention time of analytes decreases with higher temperature. But for supercritical fluid, higher temperature induces a lower density of the mobile phase, leading to an increase of the retention time [26]. The retention times of the lipids decreased with increase of flow rate of the mobile phase. Besides, the peak width also decreased (Fig. S4). The flow rate of the makeup liquid did not affect the retention times of the lipids, but it had a great influence on the peak shapes. As shown in Fig. S5, the peaks became smoother with a higher flow rate of the makeup liquid. The peak areas were increased with a higher flow rate of the makeup liquid. Because there should be sufficient time left for the second-dimension separation, the optimized conditions for the first-dimension SFC were as follows: BPR pressure, 160 bar; column temperature, 40 °C; flow rate of mobile phase, 0.4 mL/min.

In 1D SFC–MS analysis, SFC effluent is mixed with makeup fluid to ensure the ionization of analytes. As the SFC effluent flows to the interface in the 2D SFC/RPLC system, we studied whether a makeup fluid is necessary with the 2D SFC/RPLC system. Under the optimized first-dimension conditions, the flow rate of the makeup liquid was set as 0.25 and

0 mL/min. As shown in Fig. S6, LPE (17:1), AC (16:0), PC (14:1/14:1), and SM (d18:1/17:0) disappeared when the flow rate of the makeup liquid was 0.25 mL/min. Besides, the peak shape of DG (12:0/12:0) and TG (18:1/14:0/17:1) would be influenced without makeup liquid. Thus, makeup liquid was necessary for the first several fractions, and should be removed in the last several fractions. The optimized flow rate gradient of the makeup liquid is shown in Table 1, under which condition good responses were obtained for all the lipid standards.

Under the optimized conditions, 11 classes of lipids were separated into seven different fractions after first-dimension SFC (Fig. 3). The different classes of sphingolipids, including Cer, GluCer, GalCer, LacCer, and SM, were separated into different fractions, which avoided the disturbance of identification between different head groups of lipids. Although there was still coelution of different classes in the first dimension, such as DG and TG, they could be easily separated by second-dimension RPLC according to significantly different acyl chains. Thus, these results indicate the feasibility of online combination of SFC and RPLC. Compared with the NP/RP 2D LC–MS system, the analysis time is much shorter. Besides, the peak width of lipids after RPLC were much narrower than those after 1D SFC. Lee et al. [13] reported that methylation by trimethylsilyl-diazomethane could suppress peak tailing and increase the detection sensitivity of SFC–MS for diverse polar lipids, which could also be achieved by an additional dimension of RPLC separation.

Validation of the 2D SFC/RPLC–MS method

We validated the method using lipid standard mixture. The results of the analytical validation are summarized in Table 3. From these results, the correlation coefficients (R^2) were greater than 0.99 for all 11 lipid standards. Besides, the LODs ranged from 0.05 to 10 ng/mL. By our 2D SFC/RPLC–MS method, the LODs for TG (18:1/14:0/17:1), MG (17:0), and Cer (d18:1/12:0) were 0.1, 0.05, and 0.05 ng/mL, respectively. These sensitivities were 50-fold, tenfold, and tenfold higher, respectively, than those in the NP/RP 2D LC–MS method [8]. For repeatability, the RSDs of the retention time and peak area ranged from 0.00% to 0.10% and from 1.54% to 19.85%, respectively. Among these, the RSDs of the peak area for SM (d18:1/17:0), PC (14:1/14:1), and AC (16:0) were relatively high. But they were still within acceptable limits. Thus, this 2D SFC/RPLC–MS method could be applied for lipid profiling analysis in different biological or clinical samples.

Analysis of human plasma

Lipids in human plasma were separated and identified with use of the 2D SFC/RPLC–MS system. According to the MS/MS fragment patterns of each lipid class and major fatty acid composition, we optimized the MRM transition settings for each lipid species. To be specific, Cer, GluCer, GalCer, and LacCer have a similar backbone, which will yield specific

Fig. 3 Multiple reaction monitoring chromatograms of lipid standard mixture investigated by the one-dimensional supercritical fluid chromatography (SFC)–mass spectrometry (MS) method (top) and the two-dimensional SFC/reversed-phase liquid chromatography–MS method (bottom). AC acylcarnitine, Cer ceramide, DG diacylglycerol, GalCer galactosylceramide, GluCer glucosylceramide, LacCer lactosylceramide, LPE lysophosphatidylethanolamine, MG monoacylglycerol, PC phosphatidylcholine, SM sphingomyelin, TG triacylglycerol

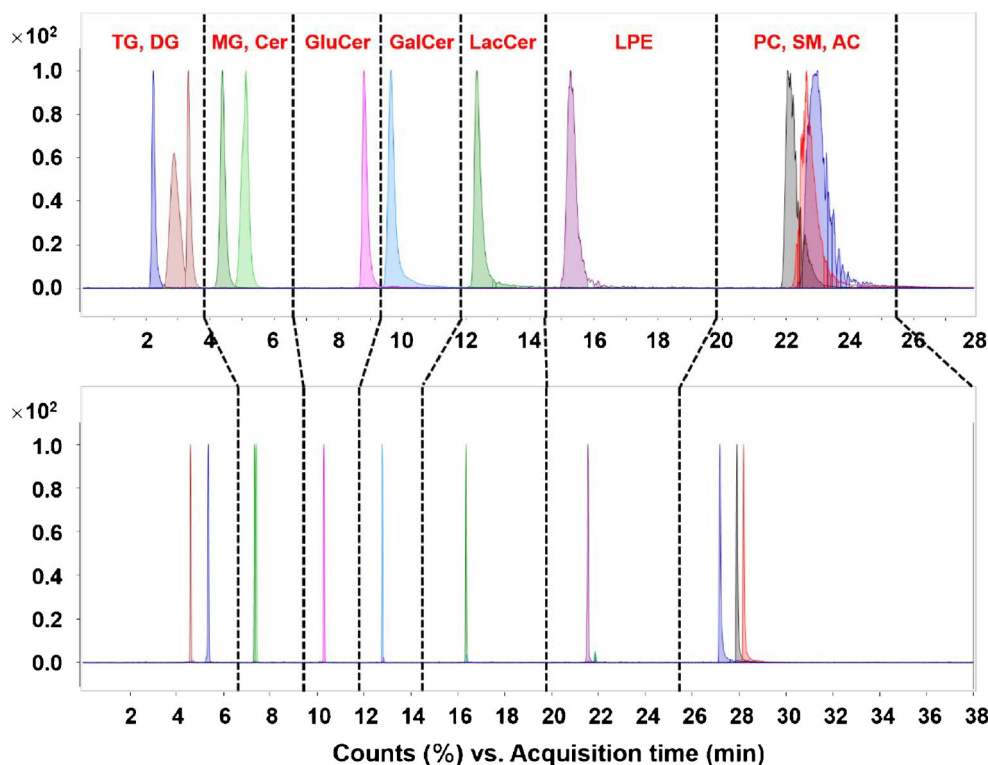


Table 3 Analytical validation of the two-dimensional supercritical fluid chromatography/reversed-phase liquid chromatography–mass spectrometry method by the determination of lipid standards

Lipid standard	Calibration equation ^a	Linear range (ng/mL)	R^2	LOD (ng/mL)	RT (min)	Area ^b	RSD (%) ($n = 6$) ^c	
							RT	Area
DG (12:0/12:0)	$y = (1.56 \times 10^5)x - 5.85 \times 10^2$	0.2–500	0.9981	0.1	4.60	1,332,239	0.00	3.77
TG (18:1/14:0/17:1)	$y = (2.79 \times 10^3)x + 4.95 \times 10$	5–500	0.9978	0.1	5.36	2949	0.03	3.27
MG (17:0)	$y = (1.13 \times 10^5)x - 5.70 \times 10$	0.1–500	0.9983	0.05	7.33	103,866	0.02	3.58
Cer (d18:1/12:0)	$y = (4.52 \times 10^5)x - 7.35 \times 10^2$	0.1–500	0.9985	0.05	7.41	409,096	0.01	1.54
GluCer (d18:1/12:0)	$y = (4.09 \times 10^4)x - 2.62 \times 10^2$	0.5–500	0.9962	0.2	10.29	42,261	0.03	2.87
GalCer (d18:1/8:0)	$y = (5.26 \times 10^4)x - 5.27 \times 10^2$	1–500	0.9940	0.1	12.78	66,980	0.01	2.44
LacCer (d18:1/8:0)	$y = (7.16 \times 10^3)x - 8.52 \times 10$	2–500	0.9943	0.2	16.35	13,826	0.03	4.43
LPE (17:1)	$y = (1.00 \times 10^3)x - 4.95 \times 10$	20–1000	0.9946	10	21.55	1516	0.10	4.84
AC (16:0)	$y = (1.84 \times 10^4)x - 3.03 \times 10^2$	20–500	0.9945	0.5	27.17	71,116	0.05	17.97
PC (14:1/14:1)	$y = (1.78 \times 10^4)x - 3.66 \times 10^2$	5–500	0.9903	1	27.91	15,610	0.00	19.58
SM (d18:1/17:0)	$y = (6.59 \times 10^3)x - 2.92 \times 10$	5–1000	0.9982	2	28.19	11,880	0.01	19.85

AC acylcarnitine, Cer ceramide, DG diacylglycerol, GalCer galactosylceramide, GluCer glucosylceramide, LacCer lactosylceramide, LOD limit of detection, LPE lysophosphatidylethanolamine, MG monoacylglycerol, PC phosphatidylcholine, RSD relative standard deviation, RT retention time, SM sphingomyelin, TG triacylglycerol

^a y represents to the peak area and x represents the concentration of the corresponding validation standard ($\mu\text{g/mL}$).

^b Obtained from the multiple reaction monitoring chromatograms.

^c 1 $\mu\text{g/mL}$

fragment ions, including ions with m/z 266.3, 264.3, and 262.4 for d18:0, d18:1, and d18:2, respectively. PC and SM have the same polar head group, which could generate ions with m/z 184.1. Besides, the specific fragment ion for AC has m/z 85.1. Thus, lipids in these classes were identified by precursor ion scan. For DG and TG, loss of RCOO^- will occur during MS/MS. Thus, we conducted a product ion scan to select the MRM transitions for lipids in these two lipid classes. LPE was monitored by the specific loss of an ion with m/z 141.0 in the neutral loss scan. Apart from this, lipid molecular species were also identified by retention times. All the retention times of the lipid species in one class were in the same fraction. In this method, a pair of isomers, GluCer and GalCer, were separated into different fractions, the retention times of which were very useful for determining the lipid species in these two classes. Besides, the relative retention time of lipid species in the same lipid class was an effective support for identification. As shown in Fig. 4a, SMs having the same double-bond number in two fatty acid chains were eluted in order of increasing total carbon number. For eight SMs with one double bond, they were eluted in the order SM (34:1), SM (36:1), SM (37:1), SM (38:1), SM (39:1), SM (40:1), SM (41:1), and SM (42:1). Besides, DGs having the same total carbon number in two fatty acid chains were eluted in the order of decreasing double-bond number. For five DGs with a carbon number of 36, they were eluted in the order DG (36:5), DG (36:4), DG (36:3), DG (36:2), and DG (36:1) (Fig. 4b). In addition, separation of isomers, for example,

GluCer (d18:1/23:0) and GluCer (d18:0/23:1), was also observed (Fig. 4c).

Finally, 370 lipid species from ten lipid classes were determined in human plasma by this 2D SFC/RPLC–QQQ MS method. The optimized acquisition settings for each lipid species, including precursor–product ion pairs, fragmentor voltage, and collision energy, are presented in Table S2. Among these lipids, some low-abundance species were successfully identified, such as GluCer (d18:1/15:1) and DG (25:4/17:0) (Fig. S7). Figure 5 shows the distribution of detected lipids in each lipid class. As we can see, the highest number of lipid species was identified for TG (81), SM (57), DG (54), PC (54), and Cer (43). Compared with 1D SFC–MS for the analysis of TGs, the number of identified TGs was similar [15]. Although more lipid classes were detected by 1D ultrahigh-performance SFC–MS [27], more lipid species in each lipid class were identified by the 2D SFC/RPLC–MS method. Thus, the 2D SFC/RPLC–MS method offered a much higher peak capacity, reduced ion suppression effects among lipid molecular species, and facilitated the identification of the lipid molecular species.

Comparison of patients with breast cancer and healthy controls

With use of this novel 2D SFC/RPLC–MS method, the differences in lipids in human plasma between patients with breast cancer ($n = 10$) and healthy controls ($n =$

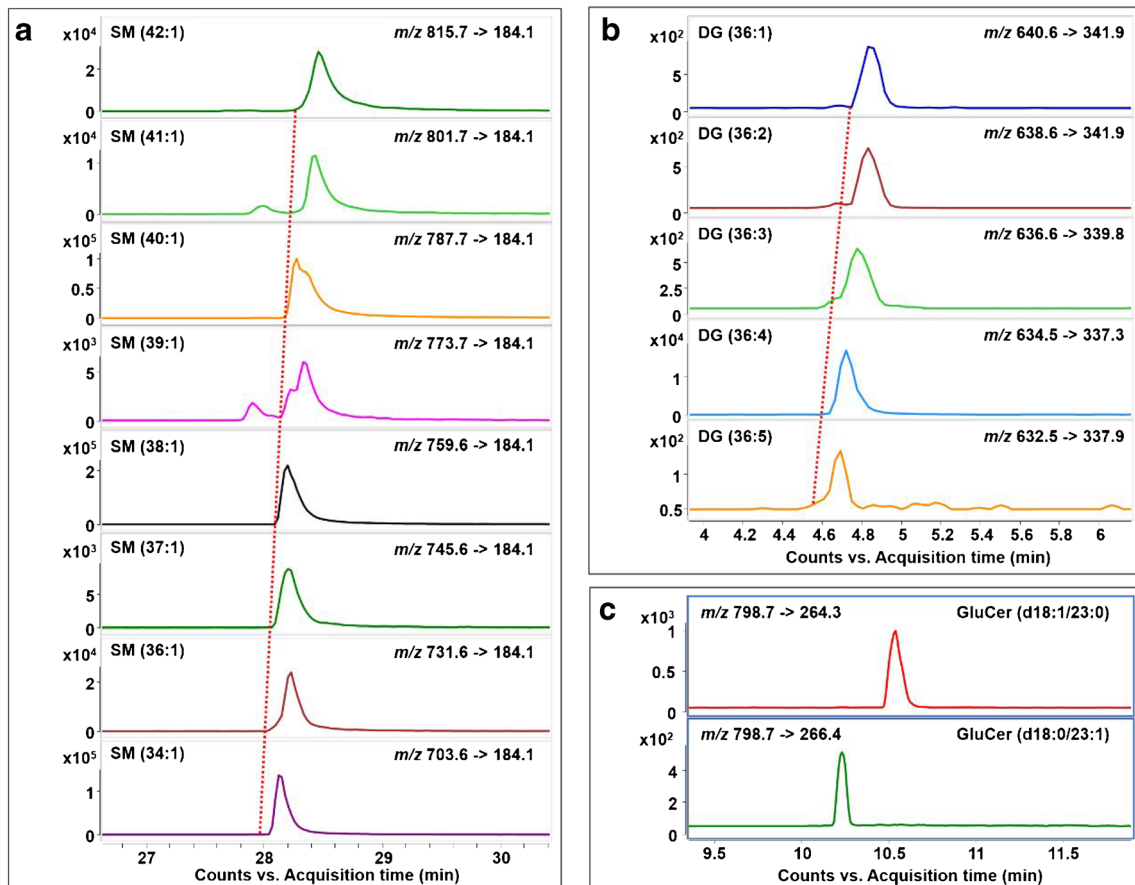


Fig. 4 Multiple reaction monitoring chromatograms of selected lipid molecular species detected by the two-dimensional supercritical fluid chromatography/reversed-phase liquid chromatography–triple-

quadrupole mass spectrometry method in human plasma. DG diacylglycerol, GluCer glucosylceramide, SM sphingomyelin

10) were explored. Among the detected lipid species, 15 TGs, 3 Cers, 1 DG, and 1 PC showed significant differences ($p < 0.05$) between the two groups. Their average corrected peak area in each group, p values, and fold

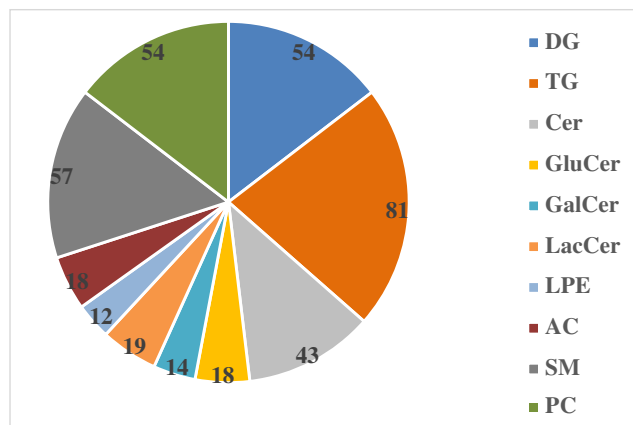


Fig. 5 Detected lipids in each lipid class in human plasma. AC acylcarnitine, Cer ceramide, DG diacylglycerol, GalCer galactosylceramide, GluCer glucosylceramide, LacCer lactosylceramide, LPE lysophosphatidylethanolamine, PC phosphatidylcholine, SM sphingomyelin, TG triacylglycerol

change are summarized in Table 4. As we can see, TGs were upregulated in the patient group, whereas Cer, DG, and PC were downregulated. They were proposed as potential lipid biomarkers for breast cancer. Among these lipids, TGs are present in the greatest number. Adipose triglyceride lipase is the rate-limiting enzyme in the TG hydrolysis cascade. A previous report showed that low levels of Adipose triglyceride lipase messenger RNA correlated with significantly reduced survival in patients with breast cancer [28], meaning TG hydrolysis was inhibited in patients with breast cancer. Consequently, TGs were upregulated, which was consistent with our results.

Conclusions

In this work, online coupling of SFC and RPLC with QQQ MS was realized for lipid profiling in human plasma for the first time. As lipid classes could be separated in the first-dimension SFC by the differences in their polarity, and lipid species could be further separated in the second-dimension RPLC according to different acyl chains of lipids in each lipid

Table 4 Detailed information of potential lipid biomarkers for breast cancer

Lipid species	Corrected peak area ^a (control)	Corrected peak area (patient)	Fold change ^b	<i>p</i> ^c
TG (16:0_18:1_24:5)	2.80 ± 1.43	2.75 ± 1.45	1.73	0.016
TG (16:0_18:2_24:5)	0.12 ± 0.07	0.22 ± 0.13	1.88	0.020
TG (18:1_18:1_22:6)	0.73 ± 0.49	1.24 ± 0.76	1.69	0.020
TG (16:0_18:0_22:5)	2.51 ± 1.35	3.94 ± 1.49	1.57	0.012
TG (16:0_18:1_22:4)	0.50 ± 0.23	0.85 ± 0.48	1.71	0.020
TG (16:0_18:1_22:5)	4.51 ± 2.32	7.89 ± 4.21	1.75	0.038
TG (20:4_18:0_18:2)	2.90 ± 0.99	4.57 ± 1.65	1.58	0.007
TG (16:0_18:2_22:5)	4.76 ± 1.92	9.42 ± 1.58	1.98	0.010
TG (18:1_18:2_20:4)	3.90 ± 1.81	5.87 ± 1.96	1.51	0.025
TG (22:6_18:2_16:0)	2.05 ± 0.91	4.28 ± 2.55	2.08	0.020
TG (18:0_18:2_19:0)	0.35 ± 0.15	0.82 ± 0.42	2.37	0.003
TG (18:1_18:2_19:1)	0.21 ± 0.15	0.40 ± 0.28	1.88	0.031
TG (16:0_18:2_20:4)	4.34 ± 1.83	7.00 ± 3.03	1.61	0.012
TG (14:0_18:1_22:6)	1.03 ± 0.61	2.20 ± 1.42	2.15	0.025
TG (14:2_18:1_18:3)	0.53 ± 0.28	0.79 ± 0.41	1.51	0.012
Cer (d18:2/24:0)	0.52 ± 0.14	0.75 ± 0.21	1.43	0.031
Cer (d18:2/22:0)	0.15 ± 0.04	0.24 ± 0.09	1.59	0.020
Cer (d18:1/21:1)	0.01 ± 0.00	0.02 ± 0.01	1.52	0.031
DG (20:0/20:0)	2.89 ± 1.53	0.48 ± 0.19	-6.04	0.000
PC (40:5)	2.58 ± 1.13	1.24 ± 0.53	-2.08	0.006

Cer ceramide, *DG* diacylglycerol, *PC* phosphatidylcholine, *TG* triacylglycerol

^a Average value for the control samples (*n* = 10) and the patient samples (*n* = 10) along with the standard deviation

^b Calculated from the arithmetic means for the patients with breast cancer and healthy controls. Fold change with a positive value indicates a relatively higher concentration in patients with breast cancer compared with the controls, whereas a negative value indicates a relatively lower concentration in patients with breast cancer compared with the controls. Data are expressed as the mean ± the standard deviation.

^c Determined by the Mann–Whitney *U* test

class, 370 lipid species from ten lipid classes were successfully identified. Besides, the sample peak broadening in the first-dimension column was suppressed, leading to high sensitivity of the method. The analysis time was significantly reduced compared with that for our previous NP/RP 2D LC–MS method (170 min). In addition, the LOD, linearity, and repeatability were satisfactory for most of the lipid standards, indicating the high sensitivity and good repeatability of this method. Finally, the method was used for the analysis of human plasma from patients with breast cancer and healthy controls. Twenty potential lipid biomarkers for breast cancer were found. From the findings taken together, the 2D SFC/RPLC–QQQ MS method shows high potential as an MS-based method in the field of lipidomics and clinical research.

Acknowledgements We thank Shaohua Zhang and Yi Liu from the Fifth Medical Center of the People's Liberation Army General Hospital for providing human plasma samples and Agilent Technologies for providing the instruments. This research was financially supported by the National Natural Science Foundation of China (no. 21527809), the National Key R&D Program of China (no. 2017YFC0906800) and the Natural Science Foundation of Shanxi Province (no. 201801D221070).

Compliance with ethical standards

Conflict of interest The authors declare that they have no competing interests.

Ethics approval All procedures performed in studies involving human participants were in accordance with the ethical standards of the institutional and/or national research committee and with the 1964 Helsinki declaration and its later amendments or comparable ethical standards.

Informed consent Informed consent was obtained from all individual participants included in the study.

References

- Gross RW, Han X. Lipidomics at the interface of structure and function in systems biology. *Chem Biol*. 2011;18(3):284–91. <https://doi.org/10.1016/j.chembiol.2011.01.014>.
- Fahy E, Subramaniam S, Murphy RC, Nishijima M, Raetz CRH, Shimizu T, et al. Update of the LIPID MAPS comprehensive classification system for lipids. *J Lipid Res*. 2009;50:S9–S14. <https://doi.org/10.1194/jlr.R800095-JLR200>.

3. Han X. Lipidomics for studying metabolism. *Nat Rev Endocrinol*. 2016;12(11):668–79. <https://doi.org/10.1038/nrendo.2016.98>.
4. Li M, Yang L, Bai Y, Liu H. Analytical methods in lipidomics and their applications. *Anal Chem*. 2014;86(1):161–75. <https://doi.org/10.1021/ac403554h>.
5. Wang J, Wang C, Han X. Tutorial on lipidomics. *Anal Chim Acta*. 2019;1061:28–41. <https://doi.org/10.1016/j.aca.2019.01.043>.
6. Sandra K, Pereira AdS, Vanhoenacker G, David F, Sandra P. Comprehensive blood plasma lipidomics by liquid chromatography/quadrupole time-of-flight mass spectrometry. *J Chromatogr A*. 2010;1217(25):4087–99. <https://doi.org/10.1016/j.chroma.2010.02.039>.
7. Hutchins PM, Barkley RM, Murphy RC. Separation of cellular nonpolar neutral lipids by normal-phase chromatography and analysis by electrospray ionization mass spectrometry. *J Lipid Res*. 2008;49(4):804–13. <https://doi.org/10.1194/jlr.M700521-JLR200>.
8. Li M, Tong X, Lv P, Feng B, Yang L, Wu Z, et al. A not-stop-flow online normal-/reversed-phase two-dimensional liquid chromatography-quadrupole time-of-flight mass spectrometry method for comprehensive lipid profiling of human plasma from atherosclerosis patients. *J Chromatogr A*. 2014;1372:110–9. <https://doi.org/10.1016/j.chroma.2014.10.094>.
9. Yang L, Cui X, Zhang N, Li M, Bai Y, Han X, et al. Comprehensive lipid profiling of plasma in patients with benign breast tumor and breast cancer reveals novel biomarkers. *Anal Bioanal Chem*. 2015;407(17):5065–77. <https://doi.org/10.1007/s00216-015-8484-x>.
10. Yang L, Lv P, Ai W, Li L, Shen S, Nie H, et al. Lipidomic analysis of plasma in patients with lacunar infarction using normal-phase/reversed-phase two-dimensional liquid chromatography-quadrupole time-of-flight mass spectrometry. *Anal Bioanal Chem*. 2017;409(12):3211–22. <https://doi.org/10.1007/s00216-017-0261-6>.
11. Yang Y, Liang Y, Yang J, Ye F, Zhou T, Li G. Advances of supercritical fluid chromatography in lipid profiling. *J Pharm Anal*. 2019;9(1):1–8. <https://doi.org/10.1016/j.jpha.2018.11.003>.
12. Yamada T, Uchikata T, Sakamoto S, Yokoi Y, Nishiumi S, Yoshida M, et al. Supercritical fluid chromatography/Orbitrap mass spectrometry based lipidomics platform coupled with automated lipid identification software for accurate lipid profiling. *J Chromatogr A*. 2013;1301:237–42. <https://doi.org/10.1016/j.chroma.2013.05.057>.
13. Lee JW, Nishiumi S, Yoshida M, Fukusaki E, Bamba T. Simultaneous profiling of polar lipids by supercritical fluid chromatography/tandem mass spectrometry with methylation. *J Chromatogr A*. 2013;1279:98–107. <https://doi.org/10.1016/j.chroma.2013.01.020>.
14. Qu S, Du Z, Zhang Y. Direct detection of free fatty acids in edible oils using supercritical fluid chromatography coupled with mass spectrometry. *Food Chem*. 2015;170:463–9. <https://doi.org/10.1016/j.foodchem.2014.08.043>.
15. Lee JW, Nagai T, Gotoh N, Fukusaki E, Bamba T. Profiling of regioisomeric triacylglycerols in edible oils by supercritical fluid chromatography/tandem mass spectrometry. *J Chromatogr B*. 2014;966:193–9. <https://doi.org/10.1016/j.jchromb.2014.01.040>.
16. Matsubara A, Bamba T, Ishida H, Fukusaki E, Hirata K. Highly sensitive and accurate profiling of carotenoids by supercritical fluid chromatography coupled with mass spectrometry. *J Sep Sci*. 2009;32(9):1459–64. <https://doi.org/10.1002/jssc.200800699>.
17. West C, Lesellier E. Characterisation of stationary phases in subcritical fluid chromatography by the solvation parameter model II. Comparison tools. *J Chromatogr A*. 2006;1110(1-2):191–9. <https://doi.org/10.1016/j.chroma.2006.02.002>.
18. Stevenson PG, Tarafder A, Guiochon G. Comprehensive two-dimensional chromatography with coupling of reversed phase high performance liquid chromatography and supercritical fluid chromatography. *J Chromatogr A*. 2012;1220:175–8. <https://doi.org/10.1016/j.chroma.2011.11.020>.
19. Sarrut M, Corgier A, Cretier G, Le Masle A, Dubant S, Heinisch S. Potential and limitations of on-line comprehensive reversed phase liquid chromatography × supercritical fluid chromatography for the separation of neutral compounds: An approach to separate an aqueous extract of bio-oil. *J Chromatogr A*. 2015;1402:124–33. <https://doi.org/10.1016/j.chroma.2015.05.005>.
20. Sun M, Sandahl M, Turner C. Comprehensive on-line two-dimensional liquid chromatography × supercritical fluid chromatography with trapping column-assisted modulation for depolymerised lignin analysis. *J Chromatogr A*. 2018;1541:21–30. <https://doi.org/10.1016/j.chroma.2018.02.008>.
21. Iguiniz M, Corbel E, Rogues N, Heinisch S. On-line coupling of achiral reversed phase liquid chromatography and chiral supercritical fluid chromatography for the analysis of pharmaceutical compounds. *J Pharm Biomed Anal*. 2018;159:237–44. <https://doi.org/10.1016/j.jpba.2018.06.058>.
22. François I, Sandra P. Comprehensive supercritical fluid chromatography × reversed phase liquid chromatography for the analysis of the fatty acids in fish oil. *J Chromatogr A*. 2009;1216(18):4005–12. <https://doi.org/10.1016/j.chroma.2009.02.078>.
23. Folch J, Lees M, Stanley GHS. A simple method for the isolation and purification of total lipids from animal tissues. *J Biol Chem*. 1957;226(1):497–509.
24. Li M, Feng B, Liang Y, Zhang W, Bai Y, Tang W, et al. Lipid profiling of human plasma from peritoneal dialysis patients using an improved 2D (NP/RP) LC-QToF MS method. *Anal Bioanal Chem*. 2013;405(21):6629–38. <https://doi.org/10.1007/s00216-013-7109-5>.
25. Ding K, Xu Y, Wang H, Duan C, Guan Y. A vacuum assisted dynamic evaporation interface for two-dimensional normal phase/reverse phase liquid chromatography. *J Chromatogr A*. 2010;1217(34):5477–83. <https://doi.org/10.1016/j.chroma.2010.06.053>.
26. Novakova L, Perrenoud AG-G, François I, West C, Lesellier E, Guillaume D. Modern analytical supercritical fluid chromatography using columns packed with sub-2 μm particles: a tutorial. *Anal Chim Acta*. 2014;824:18–35. <https://doi.org/10.1016/j.aca.2014.03.034>.
27. Lisa M, Holcapek M. High-throughput and comprehensive lipidomic analysis using ultrahigh-performance supercritical fluid chromatography-mass spectrometry. *Anal Chem*. 2015;87(14):7187–95. <https://doi.org/10.1021/acs.analchem.5b01054>.
28. Al-Zoughbi W, Pichler M, Gorkiewicz G, Guertl-Lackner B, Haybaeck J, Jahn SW, et al. Loss of adipose triglyceride lipase is associated with human cancer and induces mouse pulmonary neoplasia. *Oncotarget*. 2016;7(23):33832–40. <https://doi.org/10.18632/oncotarget.9418>.

Publisher's note Springer Nature remains neutral with regard to jurisdictional claims in published maps and institutional affiliations.